American Journal of Applied Sciences 4 (10): 807-814, 2007
ISSN 1546-9239

Contribution of the Entropy Function to the Study of Collimator for Nuclear Medicine Imaging

[1]M. S. Bouhdima, [1]I. Ellouni and [2]M. H. Ben Ghozlen
[1]Team of Physics and Medicals Technology
[2]Laboratory of Physical of Materials
University of Sfax - Faculty of Science BP 802 - 3018 Sfax- Tunisia

Abstract: Scintigraphic image currently used in the diagnosis or the evaluation process of tissues, is strongly dependant on several technical parameters specially collimator characteristics. The present work describes a numerical method, based on entropy function, able to specify depth and hole diameter of collimator as well as other geometrical parameters to get a better accuracy in scintigraphy evaluation. From the classical form of the entropy function, the entropy associated with a scintigraphic acquisition has been established. Its explicit expression includes collimator characteristics and source-collimator distance. The obtained numerical results and the performed illustrations explain the interest of the entropic approach, which takes into account both multiplex effect, counting process and spatial uncertainty. Acquisitions obtained on two kinds of collimator (general use and high resolution) by use of an uniform radioactive source, confirm the efficiency of such method in the choice of appropriate collimator.

Key words: collimator, γ - camera, entropy, noise.

INTRODUCTION

It is well known that gamma camera is still frequently used in nuclear medicine either human or veterinary [1-8]. Gamma camera devices include mainly the collimator, the crystal detector and photomultiplier; such elements are decisive for monophotonic imagery technique. However, the study of its performances remains a difficult task, because several parameters operate together. Previous works reported in the literature, take into account mainly the uncertainty relative to the detection process, the uncertainty calculation is achieved in a classical way from the averaged quadratic deviation of the fluctuating response [9-15]. It is noted that the aspects related to the collimator and its impact on the scintigraphic image quality are still untreated.

Classically, the signal to noise ratio associated with each pixel is defined by the ratio of a pixel estimation value on the corresponding quadratic deviation. This point of view must be revised, when one is interested in scintigraphic images where the occupancy rate is particularly low. The present work brings a new evaluation method based on the entropy function of a system. This method is an extended one, it includes the counting noise, the multiplex effect and the spatial uncertainty, all these parameters may be responsible for the deterioration of the acquisition quality. Accordingly collimator characteristics are introduced in the entropy function, hence the relationship between gamma camera devices and scintigraphic images is elucidated.

The present approach does not include diffusion effect, attenuation effect, septal penetration and incidental photons energy.

In the second section the implicit form of the entropy function associated with a scintigraphic acquisition is obtained.

The third section is devoted to a brief description of the gamma camera with a particular attention to the uniform radioactive source.

The results are detailed in the fourth section, the explicit entropy expressions according to the acquisition parameters, is established from simulation process. At this level, it will be checked that multiplex effect is dominating.

Corresponding Author: Mohamed Shili Bouhdima, Equipe de Physique & Technologie Médicales (EPTM), Université de Sfax, Faculté des Sciences BP 802 - 3018 Sfax- Tunisie, Tel: +21675391106, Fax: +216 74 274 437

MATERIALS AND METHOD

The entropy E, associated with a system which can have L states, whose formula can be obtained from most theory of information texts. Eq. (1) shows that it can be calculated as follows [16]:

$$E = \sum_{i=1}^{L} p_i \ln\left(\frac{1}{p_i}\right) \quad (1)$$

where E is the entropy, ln is the means natural logarithm, p_i the probability of state i.

The entropy associated with a scintigraphic acquisition utilizes three effects which will contribute to the final noise [17]: the multiplex effect, spatial uncertainty and counting noise.

These three effects are governed by the following parameters: the crystal detector intrinsic resolution R_i, the collimator sensitivity ρ, the object source parameters (depth D, width of voxel v, photon density n brought into volume unit) and finally the collimator parameters (hole length p, hole diameter d and thickness septa t).

As Fig. 1 show, the multiplex volume defined by the cone trunk (spotted zone). This volume is divided into m voxels (the voxel is a unit volume), which emit a total of N photons. The source described as a set of voxels, is characterized by N_{max} possible configurations given by Eq (2):

$$N_{max} = C^{N}_{N+m-1}. \quad (2)$$

where N is total number of photons emitted, m the voxel number of the multiplex volume.

Assuming that all configurations have the same probability $1/N_{max}$ the entropy function can be deduced in term of N_{max} : $E= \ln(N_{max})$. This assumption is adopted to make the entropy approach compatible with the high noise of any scintigraphic acquisition .When only one configuration exists, there is no entropy and the noise disappears. The other situation corresponds to the case where all configurations have the same probability, the entropy becomes maximal. For an intermediary case the entropy is medium.

The uncertainty on the definition of this volume is principally due to the crystal intrinsic resolution finished. Indeed, photons located in a point detector can come from a zone of the object more important than the multiplex volume. On the other hand, photons emitted in the multiplex volume, have more opportunity to be collected. One calculates these two extreme volumes (m_{min} and m_{max}) easily by the trunk cones volumes illustrated on the Fig. 2.

This spatial uncertainty is defined by the difference m_{max} - m_{min}. By adopting the equiprobability of multiplex volumes, the probability law P(m) associated with volume (m) will then be (3) :

$$P(m) = \frac{1}{m_{max} - m_{min}} \quad (3)$$

where m is the multiplex volume (measured in voxel), m_{max} the maximal volume emitting photons that can be collected, m_{min} the multiplex volume emitting photons that have more opportunity to be collected.

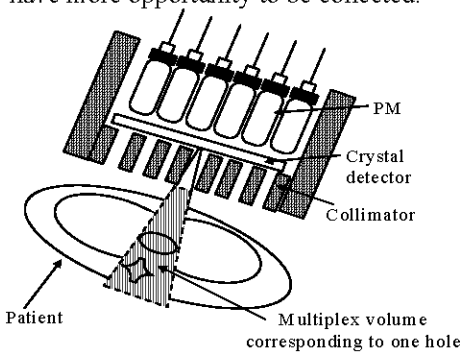

Fig. 1: Description of multiplex volume

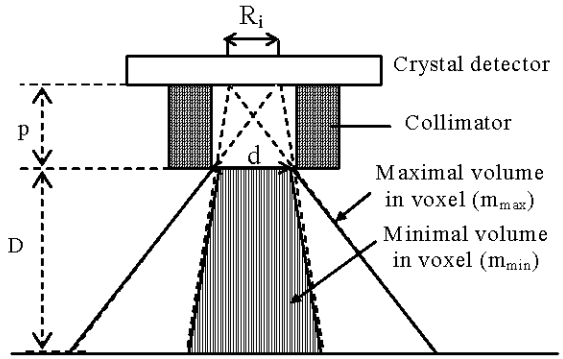

Fig. 2: Detection volume corresponding to one hole

Including multiplex effect and spatial uncertainty, the entropy formula becomes (Eq 4):

$$E = \sum_{m_{min}}^{m_{max}} P(m) \ln\left(\frac{C^{N}_{N+m-1}}{P(m)}\right) \quad (4)$$

The sensitivity is a measure of the ratio of photons emitted (N) from a point source to photons penetrating a collimator (N_d). This means that a maximum sensitivity value would mean no collimator at all (a collimator made up only of a hole) and a sensitivity value of zero corresponds to no penetration at all (a collimator with no holes). This sensitivity can be

calculated according to collimator parameters as follows (Eq 5):

$$\rho = k\left(\frac{d}{p}\right)^2\left(\frac{d}{d+t}\right)^2 \quad (5)$$

where d the collimator hole diameter (mm), p the collimator hole length (collimator thickness) (mm), t is the thickness of the septa (mm), k the numeric coefficient (equal to 0.26 for the hexagonal holes).

The probability associated with N_d detected photons, is obeying Poisson law noted $Pois(N_d)$ [18]:

$$Pois(N_d) = \frac{\overline{N}_d^{N_d}}{N_d!}\exp(-\overline{N}_d) \quad (6)$$

The entropy function being additive, its formula including previous effects and dependence on the acquisition parameters E(p,d,D,R_i,n,v) is given by [17]:

$$E = \sum_{m_{min}}^{m_{max}} \sum_{N=0}^{+\infty} Pois(N_d)\, P(m) \ln\left[\frac{C_{N+m-1}^{N}}{P(m)\, Pois(N_d)}\right] \quad (7)$$

The volume used in nuclear medicine is the average volume that can be defined by (Eq 7):

$$m_{moy} = \frac{m_{max} + m_{min}}{2} \quad (8)$$

When adopting this hypothesis the spatial uncertainty vanishes and the function to minimise will then be (Eq 9):

$$E = \sum_{N=0}^{\infty} Pois(N_d) \ln\left[\frac{C_{N+m_{moy}-1}^{N}}{Pois(N_d)}\right] \quad (9)$$

By developing the preceding result E, one can extract two factors:

- Multiplex entropy:

$$E_M = \sum_{N=0}^{\infty} Pois(N_d) \ln\left[C_{N+m_{moy}-1}^{N}\right] \quad (10)$$

- Counting entropy:

$$E_C = \sum_{N=0}^{\infty} Pois(N_d) \ln\left[\frac{1}{Pois(N_d)}\right] \quad (11)$$

The simulation method applied to the acquisition scintigraphic entropy E, is given in appendix. A software in Maple language was developed to calculate the various intermediary results. Investigations are focused on the collimator parameters and source-collimator distance.

MATERIALS AND METHOD

As mentioned previously, in nuclear medicine imaging, the investigations are often focused on volume data (patient is the emitter object), however the present work is dealing with sources whose thickness is very small compared to D the distance separating the collimator from the source. In that case, the voxels are no more three-dimensional, therefore they transform into pixels. To serve this purpose, the entropy was used. The experimental set available in France (Service of Nuclear Medicine of the hospital Hautepierre, trasbourg), is supplied with two kinds of gamma camera 'argus adac' and 'siemens'. Both cameras are provided with two collimators (general use GU, high resolution HR). The characteristics of collimators utilized during measurements, are reported in table1. The R_i parameter informs on the intrinsic resolution, which depends only on the crystalline detector.

Table 1: The parameters of the four gamma cameras

Collimators	Hole diameter d(mm)	Collimator thickness p(mm)	Septum t(mm)	intrinsic resolution R_i(mm)
Adac GU	2.95	48	1.114	3.5
Siemens GU	3	40.6	1.14	3.8
Adac HR	1.4	32.8	0.152	3.5
Siemens HR	1.11	24.05	0.16	3.8

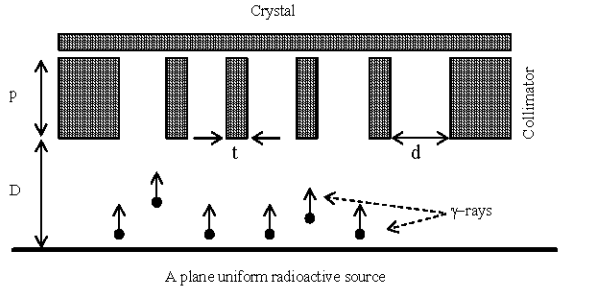

Fig. 3: Acquisition of a plane uniform radioactive source

A uniform radioactive cobalt source is located at D distance, which varies from 10 to 216mm. The entropy calculation described in the previous section, apply without important change. The only difference comes owing to the fact that the intrinsic resolution is higher than the holes diameter. To obtain the maximal multiplex volume, it is necessary to count the participation of several holes.

Figure 3 clarifies aspects related with the geometry of both the collimator and the radioactive source.

For each image a histogram is plotted, it gives an idea about acquisition quality and standard deviation named σ. The non-uniformity coefficient is taken equal to the ratio σ/n_p (where n_p is the mean photonic count relative to one pixel).

The performed simulations have been carried out on PC equipped with an INTEL Pentium 4 CPU 2.40 GHz.

Table 1: The parameters of the four gamma cameras

Collimators	Hole diamter d(mm)	Collimator thickness p(mm)	Septum t(mm)	intrinsic resolution R_i(mm)
Adac GU	2.95	48	1.114	3.5
Siemens GU	3	40.6	1.14	3.8
Adac HR	1.4	32.8	0.152	3.5
Siemens HR	1.11	24.05	0.16	3.8

Table 2: E_1 and E_2 entropy with their corresponding machine time t_1 and t_2 *: a few days

Collimators	D(mm)	10	16	110	116	210	216
Adac (GU)	E_1	16.334	33.732	766.134	851.813	3292.419	3503.934
	E_2	3.682	6.817	77.714	82.429	236.909	242.887
	t_1(s)	0.1	0.1	69.4	72.5	2116.2	*
	t_2(s)	0.1	0.1	0.1	0.1	0.8	0.8
Adac (HR)	E_1	1.613	12.577	334.669	375.904	1501.193	1604.669
	E_2	0.354	2.370	31.466	34.023	103.976	107.972
	t_1(s)	0.1	0.1	9.6	42.2	1531.4	*
	t_2(s)	0.01	0.01	0.01	0.01	1.7	2.3
Siemens (GU)	E_1	20.767	38.484	950.49	1070.92	4000..215	4340.254
	E_2	7.085	9.79	96.139	106.919	298.939	329.114
	t_1(s)	0.01	0.01	70.1	79.9	4295.6	*
	t_2(s)	0.01	0.01	0.1	0.1	0.1	0.1
Siemens (HR)	E_1	6.875	21.434	622.484	835.763	3134.258	3433.366
	E_2	1.613	4.038	68.256	80.027	226.720	235.755
	t_1(s)	0.01	0.01	66.1	70.9	4195.2	*
	t_2(s)	0.01	0.01	0.1	0.1	0.1	0.1

Table 3: Counting entropy E_C and multiplex entropy E_M values

Collimators	D(mm)	10	16	110	116	210	216
Adac HR	E_M	0	5.476	420.058	474.858	2011.006	2155.111
	E_C	1.504	1.613	2.017	2.051	2.316	2.333
Siemens HR	E_M	0	16.306	1095.834	1252.251	5742.5	6159.435
	E_C	1.613	1.734	2.299	2.342	2.596	2.604

RESULTS AND DISCUSSION

The measurements are performed for different samples and various collimators mounted at variable distance from the source. Detailed results concerning the entropy E ones are presented in table form. The obtained results E will be compared to classical parameters associated with scintigraphic image quality as the ratio signal on noise SNR, spatial resolution R_s and sensitivity ρ.

Simulation: The simulations based on entropy, include multiplex, counting effects and spatial uncertainty. By application of equations (7, 9), global entropy has been computed. Table 2 contains both E_1 (Eq 7) and E_2 (Eq 9) entropy with their corresponding machine time, for the available densities. In addition, the table (3) presents the values of counting entropy E_C and those of the multiplex entropy E_M according to D. This table shows that the multiplex effect is more dominant than counting effect for more important D. For an average volume $m_{moy} \leq 1$ voxel (for $D \leq 10$mm in this case), the multiplex entropy (E_M) is equivalent to zero.

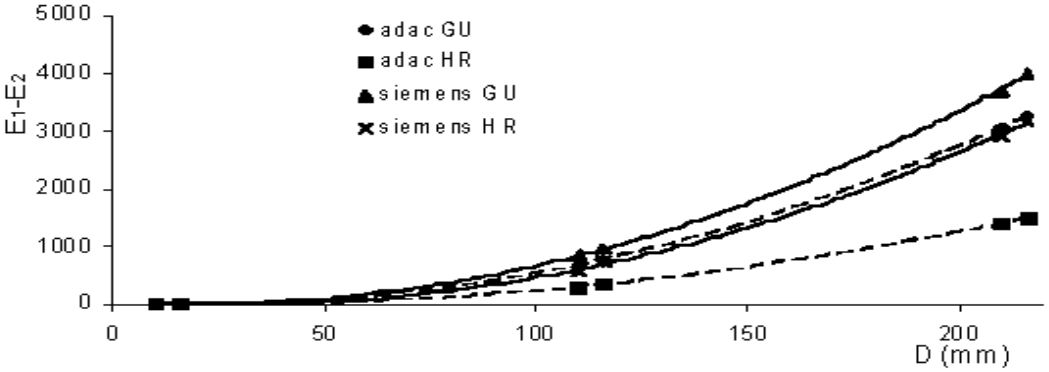

Fig. 4: Variation of ΔE according to D for different collimator

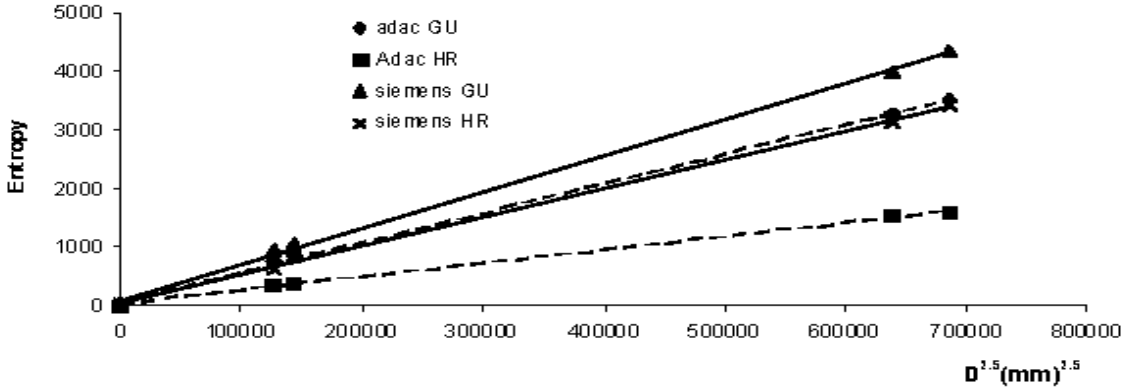

Fig. 5: E_2 entropy variation according to $D^{2.5}$ for different collimator

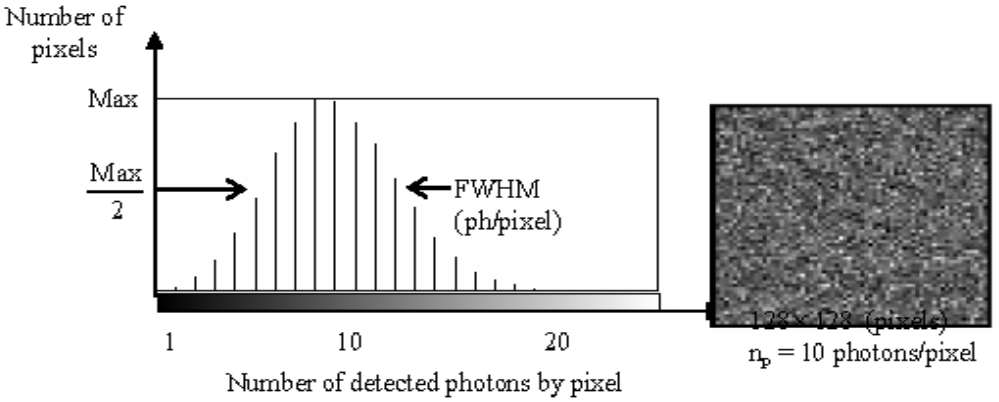

Fig. 6: The number of pixels versus the number of detected photons by pixel_for uniform source (images acquired with a collimator Adac HR for D=10mm)

The data is presented in two groups of plots; each group has four plots (Fig. 4, 5). Although difference $E_1 - E_2$ is large for a variety of source-collimator distance D; The plot $\Delta E=E_1 - E_2$ versus D (as shown in Fig. 4) shows that the spatial uncertainty effect is desirable when D is the lowest. That is why E_2 entropy can be retained instead of E_1 entropy to characterize scintigraphic images. In addition, machine time is considerably saved during E_2 calculation mainly when D increases. Thus, in using these results, the first decision to make is to be used E_2 instead of E_1 in the case of scintigraphic image where D is not important.

Approximate Expression of The Entropy E: From the values simulated of E obtained above corresponding to D, the fitting curve reveals that E can be written as follows:

$$E^i(D) = a_i\ D^{2.5} + b_i \quad (12)$$

While D exponent is always equal to 2.5, the a_i and b_i coefficients are dependent on collimator parameters. The plot reported in Fig. 5, confirms the linear variation of E in term of $D^{2.5}$. The values of coefficients are summarized in table (4).

Table 4: a_i and b_i coefficients values

	Adac GU	Adac HR	Siemens GU	Siemens HR
$a_i\ 10^{-4}$	3	2	4	4
b	17.91	6.16	22.55	13.07

In addition, it is checked that $a_i\ p^{4/3}$ and $b_i\ p^{4/3}$ vary in linear manner according to d^2, so explicit formula can be written:

$$a_i\ p^{4/3}=(46\ d^2+130)\ 10^{-4} \quad (13)$$

$$b_i\ p^{4/3} = 315\ d^2 + 300 \quad (14)$$

The analytical form of E(D,d,p) becomes as follows:

$$E=\left[\frac{(46\ d^2+130)10^{-4}}{p^{4/3}}\right] D^{2,5} + \frac{315\ d^2+300}{p^{4/3}} \quad (15)$$

As this formula shows, the good value of E is obtained by using small - hole diameters, bringing the collimator as close as possible to the source, and using a thick slab of lead. The explicit form of entropy (Eq 15) is useful to make an optimal choice of acquisition and collimator parameters, one has to remind that decreasing E permits to get best scintigraphic images.

Analysis of Scintigraphic Images: With JAVA IMAGE J, we analysed the uniform source images acquired by various collimators for different values of D. All of them are characterized by a non uniform histogram; the number of detected photons varies from one pixel to another. Each histogram gives the number of pixels (Y-axis) with respect to the number of detected photons by pixel (X-axis). The plot reported in Fig. 6, presents the histogram and image acquired by adac HR collimator (for D=10mm in this case).

As this Fig. shows, the standard deviation named 2σ can be appraised by the FWHM (full width at half maximum) of the histogram. Similar conclusions can be obtained in the other cases; the results are summarized in table (5).

This makes up a method to characterize the noise (σ) and obtain the non-uniformity coefficient (which is taken equal to the ratio σ/n_p). So we can see that for all these acquisitions the noise exists. The question is in which way the noise is related to the entropy to have an idea about the image quality.

The parameters associated with scintigraphic image quality mainly signal-noise ratio, spatial resolution, sensitivity, σ/n_p ratio and entropy are reported in table 5. By reading these values, scintigraphic images may be compared to each other.

DISCUSSIONS

At present, the images obtained in monophotonic imagery, have a poor space resolution (10 mm) and a low sensitivity (10^{-4}) but they are still utilised and exploited for their dynamic characters[5,7]. Moreover, the image quality seems to be extremely dependent on collimator geometry and distance source-collimator[19-24].

Figure 4 as well as table 2, show that E_1 entropy (Eq 7) and E_2 entropy (Eq 9) have the same behavior according to the distance source-collimator (D) with an advantage in the machine time. This result reveals that E_1 entropy can be replaced by E_2 one which is easier to be computed. The access to E_2 value and the knowledge how it evolves may be precious during collimator design. The explicit form of entropy (Eq 15) according to the acquisition parameters: D, p, and d, is worth to be reviewed and eventually improved by new acquisitions. The purpose of this formula is to assist the investigator to decide which acquisition parameters to use.

Up to now, the image quality is estimated separately through the acquisition parameters, the entropy seems to be the unique function where these parameters exist together. Then the impact on quality due to any change in parameters can be valued from the entropy variation. Assuming an experiment with the same collimator, the entropy and σ/n_p vary in the same direction with respect to D. Therefore decreasing D is the best mean to

improve the image quality. The collimator's previous works[19-22,25-31], based on the estimate of the impulse response lead to study only the spatial resolution, the sensitivity and septal transparency. However from table 4 and by comparing cameras equipped with HR collimator, one notices that the sensitivity is in favour of Siemens camera ($1.1\ 10^{-4}$ against 10^{-4}) whereas the spatial resolution is in favour of Adac camera (3.94 mm against 4.225 mm). Adac images are better since the ratio σ/n_p is lower; this result is coherent with the entropy. It is noted that new acquisition parameters as internal photon density n, intrinsic resolution R_i and voxel dimension v, have to be included to get a generalized form of the entropy method.

CONCLUSION

The scintigraphic acquisition entropy was introduced to analyze the noise in gamma camera images. The entropy is formulated on the basis of collimator characteristics as well as source parameters.

The image quality related to a uniform source has been studied by the entropy method. It was demonstrated that it is in agreement with the histogram analysis. Thus, the obtained explicit form of the entropy inquires about scintigraphic image quality. It connects simply and explicitly the entropy with the acquisition parameters. This method can be utilized instead of spatial resolution, sensitivity and SNR ratio considered together.

The acquisition entropy provides a simple tool to compare various types of gamma cameras. The optimization of the acquisition parameters will contribute to the improvement of the scintigraphic image quality.

ACKNOWLEDGEMENTS

We express our appreciation and thanks to the team of Pr. Andre Constantinesco (Service de Médicine Nucléaire, Hôpital Hautpierre, Strasbourg, France).
We wish to thank Mme Flah Latifa for her review of English on previous versions of the manuscript.

REFERENCES

1. F.J. Beekman, C. Kamphuis, M.A. King, P.P. van Rijk and M.A. Viergever, 2001. Improuvement of image resolution and quantitative accuracy in clinical Single Photon Emission Computed Tomography: Computerized Medical Imaging and Graphics, 25 (2): 135-146.
2. FJ. Beekman and B. Vastenhouw, 2004. Design and simulation of a high-resolution stationary SPECT system for small animals: Phys. Med. Biol., 49 (19): 4579-4592.
3. P. Barthez, 2004. Nuclear medicine in small animals: EMC-Vétérinaire, 1 (5): 191-198.
4. S. Craig Lvin, 2003. Detector design issues for compact nuclear emission cameras dedicated to breast imaging: Nucl. Instr. and Meth. A, 497 (1): 60-74.
5. F. Cusanno, R. Accorsi, M.N. Cinti, S. Colilli, A. Fortuna, F. Garibaldi, F. Giuliani, M. Gricia, R.C. Lanza, A. Loizzo, M. Lucentini, R. Pani, R. Pellegrini, F. Santavenere and F. Scopinaro, 2004. Molecular imaging by single-photon emission: Nucl. Instr. and Meth. A, 527: 140-144.
6. N. Flavio, V. Paolo, C. Piero, B. Francesca, G. Nicola, D. Marta, M. Guiliano and R. Guido, 2001. Clinical correlative evaluation of an iterative method for reconstruction of brain SPECT images: Nucl. Med. and Biol., 28: 627-632.
7. B. Mahmoud, M. Bedoui, R. Raychev and H. Essabbah, 2003. Conception d'un système PC-compatible d'acquisition et de traitement des images en médecine nucléaire : ITBM-RBM.,24 (5) : 267-272.
8. M. Ricard, 2004. Imaging of gamma emitters using scintillation cameras: Nucl. Instr. and Meth. A, 527: 124-129.
9. F G.E. akhri, I. Buvat, H. Benali, A. Todd-Pokropek and R. Di Paola, 2000. Relative impact of Scatter, collimator response, attenuation and finite resolution corrections in cardiac SPECT: J Nucl. Med., 41 (8): 1400-1408.
10. J.C. Gore, 1978. Statistical limitations in computed tomography: Phys. Med. Biol., 23 (6): 1176-1182.
11. R.H. Huesman, 1977. The effect of a finite number of projection angles and a finite lateral sampling of projection on the statistical errors in traverse section reconstruction: Phys. Med. Biol, 22 (3): 511-521.
12. L.A. Shepp and B.F. Logan, 1974. The Fourier reconstruction of a head section: IEEE Trans. Nucl. Sci, NS- 21: 21-43.
13. F. Soussaline, S. Houle, D. Plumer and A. Todd-Pokropek, 1979. Potentials of quantitative methods in photon emission tomography: INSERM, 88: 215-242.
14. I. Elloumi, 2002. The detection statistical theory: Applied study of the ratio signal on noise in single photon emission computed tomography: ITBM / RBM, 23 : 166-171.

15. M.J. Tapiovaara and R.F. Wagner, 1993. SNR and noise measurements for medical imaging: A practical approach based on statistical decision theory: Phys. Med. Biol., 38 (1): 71-92.
16. J. Auvray, 1979. Electronique des signaux échantillonnés et numériques. Ed. Dunod Paris, pp : 171-196.
17. I. Elloumi and J. Dammak, 2002. The acquisition scintigraphic entropy (I). Principle of bases and acquisition expression parameters. Med. Nucl., 26 (4): 189-198.
18. L .A. Shep and Y. Vardi, 1982. Maximum likelihood reconstruction for emission tomography: IEEE Transactions on Medical Imaging, Ml-1: 122-135.
19. KJ. Donohoe, R.E. Henkin, H.D. Royal, M.L. Brown, B.D. Collier, R.E. O'Mara and R.F. Carretta, 1996. Procedure guideline for bone scintigraphy: J. Nucl Med., 37: 1903-1906.
20. P. Gantet, B. Danet, J.P. Esquerré and R. Guiraud, 1990. Collimator calculation for a single slice SPECT system: Phys. Med. Biol., 35 (1): 21-32.
21. P. Gantet, P.J. Esquerre, B. Danet, G. Roux and R. Guiraud, 1990. Une méthode d'aide à la conception des collimateurs pour la médecine nucléaire: J. Med. Nuc. Biophy., 14 (2) : 129-136.
22. D.A. Podoloff, E.E. Kim and T.P. Haynie, 1992. SPECT in the evaluation of cancer patients: Radiology, 183: 305-317.
23. L. Dean, T. Andrew, K. Harry and B. Alanah, 2002. Optimisation of the design of round-hole parallel collimators for ultra-compact nuclear medicine imaging: Nucl. Instr. and Meth. A, 488: 428-440.
24. E. Tournier, C. Mestais and O. Peyret, 1994. The sensitivity-resolution compromise, collimation methods, multi-detectors cameras, tomographic methods: Med. Nucl., 18 : 317-321.
25. I. Buvat, S. Laffont, J. Lecloirec, P. Bourguet and R.D. Paola, 2001. Importance of the choice of the collimator for the detection of small lesions in scintimammography : a phantom study: Phys. Med. Biol., 46 (5): 1343-1355.
26. P. Gantet, J. P. Esquerre, B. Danet and R. Guiraud, 1990. A simulation method for studying scintillation camera collimators: Phys. Med. Biol, 35 (5): 659-669.
27. P. Gantet, R. Lagrevol, B. Danet, F. Barre and R. Guiraud, 1997. Simulation study of the influence of collimator defects on the uniformity of scintigraphic images: Phys. Med. Biol., 42 (3): 603-609.
28. N. Giocaris, G. Loudos, D. Maintas, A. Karabarbounis, V. Spanoudaki, E. Stiliaris, S. Boukis, A. Gektin, A. Boyarintsev, V. Pedash and V. Gayshan, 2004. Crystal and collimator optimization studies of a high-resolution gamma camera based on a position sensitive photomultiplier: Nucl. Instr. and Meth. A, 527: 134-139.
29. J. Maeght, 2000. Resolution in dynamic emission tomography: SIAM Journal of Mathematical Analysis, 31 (5): 1100-1120.
30. D.R. Gilland, E.L. Johnson, T.G. Turkington, R.E. Coleman and R.J. Jaszcsak, 1996. Evaluation of a Pinhole Collimator for I-131 SPECT Head Imaging: IEEE transactions on Nuclear Science, 43 (4): 2230-2238.
31. J.C. Yanch, A.B. Dobrzeniercki, C. Ramanathan and R. Berhrman, 1992. Physically realistic Monte Carlo simulation of source, collimator and Tomographic data acquisition for emission computed tomography: Phys. Med. Biol., 37 (4): 853-870.